Cascaded Random Raman Fiber Laser With Low RIN and Wide Wavelength Tunability

Bing HAN*, Shisheng DONG, Yang LIU, and Zinan WANG

Key Laboratory of Optical Fiber Sensing & Communications (Ministry of Education), University of Electronic Science and Technology of China, Chengdu 611731, China

*Corresponding author: Bing HAN E-mail: han_bing@std.uestc.edu.cn

Abstract: Cascaded random Raman fiber lasers (CRRFLs) have been used as a new platform for designing high power and wavelength-agile laser sources. Recently, CRRFL pumped by ytterbium-doped random fiber laser (YRFL) has shown both high power output and low relative intensity noise (RIN). Here, by using a wavelength- and bandwidth-tunable point reflector in YRFL, we experimentally investigate the impacts of YRFL on the spectral and RIN properties of the CRRFL. We verify that the bandwidth of the point reflector in YRFL determines the bandwidth and temporal stability of YRFL. It is found that with an increase in the bandwidth of the point reflector in YRFL from 0.2 nm to 1.4 nm, CRRFL with higher spectral purity and lower RIN can be achieved due to better temporal stability of YRFL pump. By broadening the point reflector's bandwidth to 1.4 nm, the lasing power, spectral purity, and RIN of the 4th-order random lasing at 1349 nm can reach 3.03 W, 96.34%, and –115.19 dB/Hz, respectively. For comparison, the spectral purity and RIN of the 4th-order random lasing with the point reflector's bandwidth of 0.2 nm are only 91.20% and –107.99 dB/Hz, respectively. Also, we realize a wavelength widely tunable CRRFL pumped by a wavelength-tunable YRFL. This work provides a new platform for the development of ideal distributed Raman amplification pump sources based on CRRFLs with both good temporal stability and wide wavelength tunability, which is of great importance in applications of optical fiber communication and distributed sensing.

Keywords: Random fiber laser; Raman fiber laser; relative intensity noise; distributed Raman amplification

Citation: Bing HAN, Shisheng DONG, Yang LIU, and Zinan WANG, "Cascaded Random Raman Fiber Laser With Low RIN and Wide Wavelength Tunability," *Photonic Sensors*, 2022, 12(4): 220414.

1. Introduction

Random Raman fiber lasers (RRFLs), operating via Raman gain and random distributed Rayleigh backscattering feedback in the passive fiber, have been first demonstrated in 2010. Different from conventional Raman fiber lasers, RRFLs have no well-defined resonant cavity, which is replaced by random distributed Rayleigh backscattering in fiber [1–4]. Since then, RRFLs provide a new platform for designing high power [5, 6], wavelength tunable [7, 8], linearly-polarized [9, 10], supercontinuum [11, 12], narrow linewidth [13, 14], multi-wavelength [15, 16], mid-infrared [17], and pulsed [18, 19] laser sources. With unique properties such as ultra-long cavity, good environmental insensitivity, low spatial/temporal coherence, and low noise, RRFLs have found various applications in optical fiber

Received: 14 March 2022 / Revised: 22 March 2022

DOI: 10.1007/s13320-022-0660-y
Article type: Regular

communication [20], remote sensing [21, 22], distributed sensing [23, 24], imaging [25, 26], frequency doubling [27, 28], etc.

Particularly, cascaded random Raman fiber lasers (CRRFLs) can generate high power and wavelength agile lasing beyond rare earth emission bands [2, 8, 29–37], which can find important applications in distributed Raman amplification of optical fiber communication and sensing systems. To improve the long-distance optical fiber communication and sensing systems performances, the low-noise distributed Raman pump sources are preferred. Pumped by tunable conventional ytterbium-doped fiber laser, continuously wavelength tuning covering 1 μm to 1.9 μm of CRRFL can be obtained [32]. However, with longitudinal mode beating, temporal intensity fluctuations of such a CRRFL are severe. With the help of the high power and low-noise amplified spontaneous emission (ASE) of ytterbium-doped fiber (YDF) as the pump source, the spectral purity and temporal stability of the CRRFL can be significantly enhanced [29–33]. It is also found that with the broader filtering bandwidth of the ASE source, higher spectral purity and temporal stability of the CRRFL can be realized [34]. However, wavelength tuning range of filtered ASE pump is limited due to low filtered power of ASE source with filtering wavelength beyond 1 080 nm, which further limits wavelength tuning range of CRRFL [35]. Recently, CRRFLs pumped by modeless ytterbium-doped random fiber lasers (YRFLs) have been proposed with high power and low relative intensity noise (RIN) output in a simple structure [36, 37]. Compared to conventional ytterbium-doped fiber laser and ytterbium-doped filtered ASE source, YRFL can act as a pump source for the CRRFL featuring both low-noise and wide wavelength tunability [38]. However, impacts of the YRFL pump characteristics on spectral and RIN properties of CRRFLs are still under investigation.

In this paper, we experimentally demonstrate a CRRFL with wavelength- and bandwidth-tunable YRFL pump. The influences of the point reflector's bandwidth on the bandwidth and temporal stability of the YRFL pump are first investigated, which plays an important role in the spectral and RIN properties of the CRRFL. The experimental results show that with an increase in the bandwidth of the point reflector in the YRFL from 0.2 nm to 1.4 nm, the CRRFL can have higher spectral purity and lower RIN. Furthermore, a wavelength continuously tunable CRRFL with a tunable YRFL pump is demonstrated. This work shows that the CRRFL with both good wavelength tunability and temporal stability can be achieved with the tunable broadband random lasing pump, which provides a new kind of distributed Raman amplification pump source for long-distance optical fiber sensing.

2. Experimental setup and pump properties

2.1 Experimental setup

The schematic diagram of the proposed tunable YRFL pumped CRRFL is shown in Fig. 1. For the tunable YRFL seed, as shown in the dash box of Fig. 1, light from a 976 nm laser diode (LD) is injected into a 6-m-long YDF (Nufern LMA-YDF-10/130-M) through a (2+1)×1 pump combiner. The ytterbium-doped gain in the YDF and the Rayleigh backscattering in the SMF, together with the point reflector construct a forward-pumped half-open cavity YRFL. The point reflector consists of a 1:1 coupler and a wavelength- and bandwidth-tunable filter (WL Photonics Inc., WLTF-BA-U-1 060-80-SM-0.25/1.0/00-5.0), which can determine the wavelength and bandwidth of the YRFL. The filter has a wavelength tuning range of 1 020 nm – 1 100 nm with 0.02 nm resolution and a –3 dB bandwidth tuning range of 0.20 nm – 40 nm. The power of the YRFL is further boosted in the master oscillator power amplifier (MOPA) stage which is consisted of another LD and a 10-m-long YDF. The amplified YRFL is used as the pump source for the CRRFL and is injected into a wavelength division multiplexer (WDM) (pass port:

1 040 nm – 1 095 nm, reflection port: 1 105 nm – 1 700 nm) through another isolator (ISO). The reflection port of the WDM is connected to another 1:1 coupler based wideband fiber loop mirror, providing point feedback for cascaded random Raman lasing. The common port of the WDM is spliced with a 4-km-long dispersion shifted fiber (DSF) to provide the Raman gain and random distributed Rayleigh backscattering. To generate stable 1.3 μm 4th-order random Raman lasing and avoid the unwanted nonlinear effect, the DSF with zero dispersion wavelength of 1499 nm is used here rather than the standard single-mode fiber with zero dispersion wavelength of about 1310 nm. In this way, the CRRFL is realized in a forward-pumped scheme, and the spectral and RIN properties of the CRRFL can be tailored by tuning the wavelength and bandwidth of the point reflector in the YRFL.

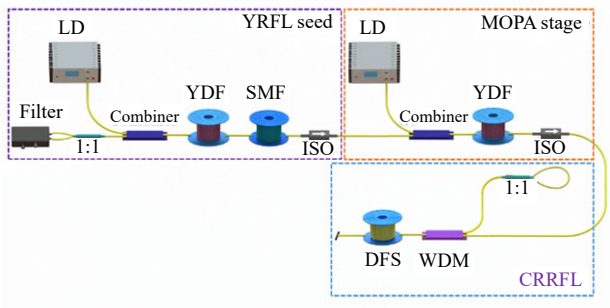

Fig. 1 Experimental setup of CRRFL pumped by tunable random lasing.

2.2 Lasing properties of the YRFL seed

First, the influence of the point reflector's bandwidth on the spectral property of the YRFL seed is investigated by tuning the bandwidth of the filter. Figure 2(a) displays the bandwidth-tunable spectra of the YRFL seeds according to the point reflector's bandwidths. The power of the YRFL seed is 0.63 W with the LD power of 4 W. The reflection bandwidth of the point reflector, which is determined by the bandwidth tunable filter, in the forward-pumped structure allows the selective gain only for the YRFL radiation [39, 40]. Thus, the bandwidth of the ytterbium-doped random lasing could be changed according to the bandwidth of the point reflector. It can be observed that the –3 dB bandwidths of the 1 085.5 nm YRFL seeds are broadened with an increase in the point reflector's bandwidth. As shown in Fig. 2(b), the –3 dB bandwidths of the YRFL seeds with 0.2 nm, 0.4 nm, 0.6 nm, 0.8 nm, 1.0 nm, and 1.4 nm of point reflector's bandwidths are 0.23 nm, 0.28 nm, 0.35 nm, 0.50 nm, 0.53 nm, and 0.65 nm, respectively. Further increasing the point reflector's bandwidth to 2 nm would result in an unstable random lasing spectrum with multi-peaks structure. This is mainly due to the existence of significant ripples in the transmission spectrum of the filter when the filtering bandwidth is beyond 2 nm. Further work can be done to realize a broader YRFL by using a ripple-free bandpass filter with the broader filtering bandwidth.

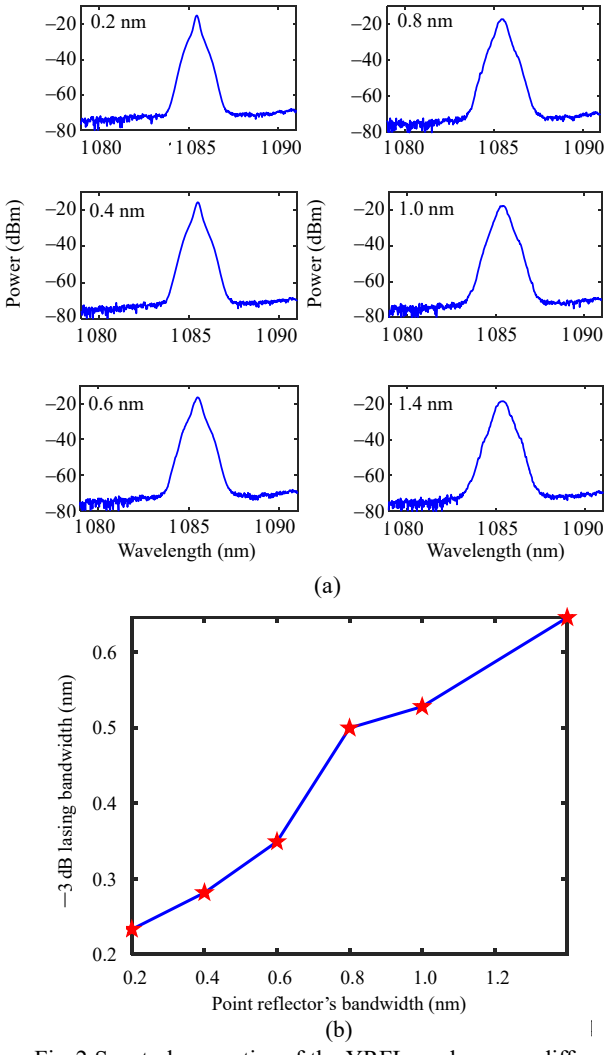

Fig. 2 Spectral properties of the YRFL seeds versus different point reflector's bandwidths: (a) spectra evolution and (b) the –3 dB bandwidths.

The temporal characteristics of the YRFL seeds versus different point reflector's bandwidths are measured by a photodetector with a 400 MHz bandwidth and an oscilloscope with a 2 GHz bandwidth. It can be seen in Fig. 3(a) that by increasing the bandwidth of the point reflector, the temporal stability of the YRFL seed can be improved. The time domain traces in a 5 ms span show that standard deviations versus mean values (STD/mean) of the YRFL seeds with 0.2 nm and 1.4 nm point reflector's bandwidths are 6.45% and 3.67%, respectively. Meanwhile, the RINs of the YRFL seeds are measured with a frequency span of 0–10 MHz and plotted in Fig. 3(b), and the RIN of the YRFL seed is lower with the broader point reflector's bandwidth. The RIN of the YRFL at 10 MHz can be decreased from –111.60 dB/Hz to –116.77 dB/Hz by increasing the bandwidth of the point reflector from 0.2 nm to 1.4 nm. The results in Figs. 2 and 3 confirm that the temporal stability of the YRFL can be improved by increasing the bandwidth of the YRFL. The temporal dynamic properties of the YRFL could be analyzed by using the non-linear Schrodinger equation (NLSE) [41, 42], which will be carried out in the future.

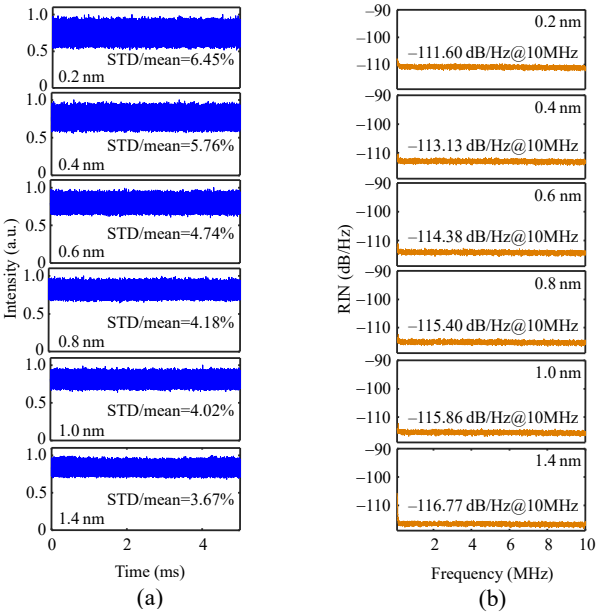

Fig. 3 Temporal properties of the YRFL seeds with different point reflector's bandwidths: (a) time domain traces and (b) RINs.

2.3 Temporal stability evolution of the amplified YRFL

We further study the temporal stability evolution of the amplified YRFL after the isolator in the MOPA stage. The measured optical conversion efficiency from the LD power to the amplified YRFL power after the isolator is 70.9%. The bandwidth of the point reflector in the YRFL seed is fixed as 1.4 nm. As presented in Figs. 4(a) and 4(b), the STD/mean and RIN of the amplified YRFL at 18 W of the LD power are only increased by 0.81% and 0.79 dB, respectively, which confirms that the temporal stability of the amplified YRFL only deteriorates slightly in the MOPA stage.

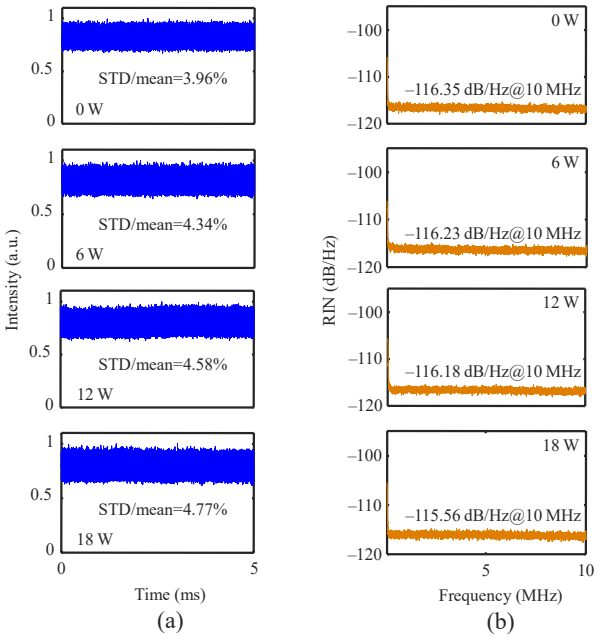

Fig. 4 Temporal properties of the amplified YRFL pumps with different LD powers: (a) time domain traces and (b) RINs.

3. Experimental results on CRRFL properties

3.1 Characterization of CRRFL pumped by random lasing

The amplified YRFL is used as the pump source for the CRRFL. By fixing the point reflector's bandwidth as 1 nm in the YRFL, the evolution of cascaded random Raman lasing is studied in this section. The spectra of the 1st- to 4th-order random lasings are illustrated in Fig. 5(a), with the amplified

YRFL pump power, which is measured after the WDM with 0.80 dB insertion loss of 2.62 W, 4.10 W, 6.07 W, and 9.03 W, respectively. With an increase in the YRFL pump power, the 1 141 nm 1st-order random lasing generates at first with an unstable behavior. Plenty of random spikes can be observed in the lasing spectrum, which could be attributed to the generation of narrow-band spectral components and the cascaded stimulated Brillouin scattering [1, 2]. By further increasing the pump power, the 2nd- to 4th-order random lasings with smooth and stable spectra can be stimulated successively. The central wavelengths of the 1st- to 4th-order random lasings are 1 141 nm, 1 207 nm, 1 275 nm, and 1 349 nm, respectively. The time domain traces of each order of random lasing are measured and shown in Fig. 5(b), corresponding to the left column of the spectra. It can be seen that, for the unstable 1st-order random lasing, it shows a pulsed scenario in time domain as well. The time domain traces of the 2nd- to 4th-order random lasings show quasi-continuous wave behaviors, and the STD/mean value increases with the order of Raman lasing.

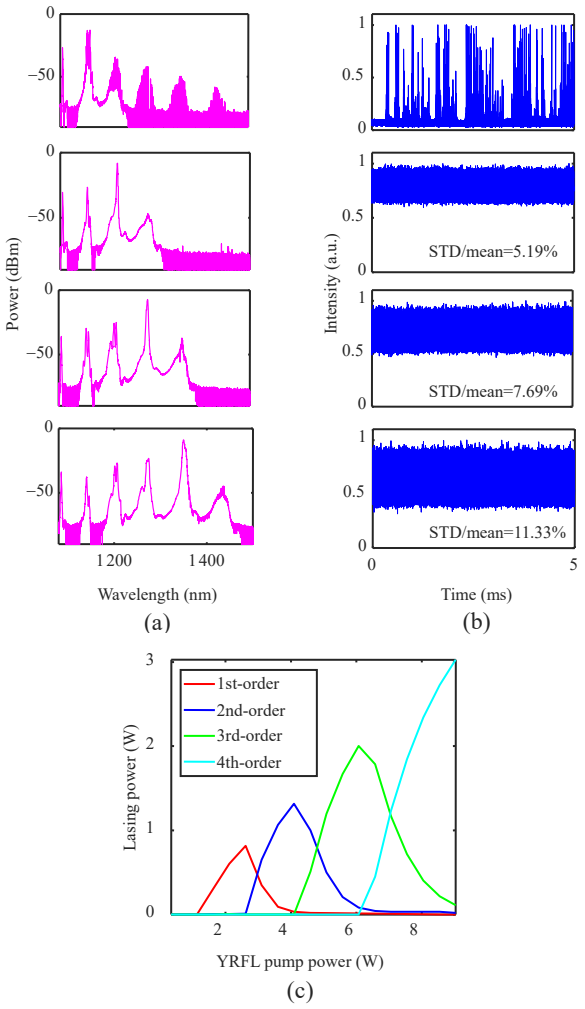

Fig. 5 Evolution of the CRRFL: (a) spectra, (b) time domain traces, and (c) lasing power.

The output power evolution of the 1st- to 4th-order random lasings is depicted in Fig. 5(c). The threshold lasing powers of the 1st- to 4th-order random lasings are 1.14 W, 2.62 W, 4.10 W, and 6.07 W, respectively. As a result, the maximum output power of the 4th-order random lasing reaches 3.03 W at the pump power of 9.03 W, corresponding to an optical conversion efficiency of 33.6%.

3.2 Influence of YRFL pump characteristics on 4th-order CRRFL

The influences of the YRFL pump on the 4th-order CRRFL are also investigated. Firstly, the spectral purities of the 4th-order random lasing, which is defined as the ratio of the output of the 4th-order random lasing to the total output, as a function of point reflector's bandwidths in the YRFL are measured and plotted in Fig. 6(a). The spectral purity of the 4th-order random lasing pumped by the YRFL with 0.2 nm of point reflector's bandwidth is only 91.20%. While, by employing a relatively broadband YRFL pump with 1.4 nm of point reflector's bandwidth, the spectral purity of the 4th-order random lasing can be improved to 96.34%. The higher spectral purity of random lasing could be associated with the lower RIN of the YRFL pump [35]. The influence of the YRFL pump on the temporal stability of the 4th-order random lasing is also measured and presented in Fig. 6(b). It can be seen that with the broader YRFL pump, the temporal stability of the 4th-order random lasing can be enhanced. This is due to the temporal intensity fluctuation of the pump is transferred directly to the CRRFLs by the ultra-fast responding process of the stimulated Raman scattering effect [43]. As a result,

the time domain STD/mean value of the 4th-order random lasing decreased from 20.74% to 10.81% by increasing the bandwidth of the point reflector in the YRFL from 0.2 nm to 1.4 nm. Meanwhile, the RIN spectra of the 4th-order random lasing in Fig. 6(c) also verify that the RIN of the 4th-order random lasing can be decreased by 7.2 dB with the broader YRFL pump. The results illustrated in Fig. 6 show that the YRFL pump bandwidth has a significant effect on the lasing performances of the CRRFL, due to the different temporal stability behaviors of the YRFLs under different bandwidths.

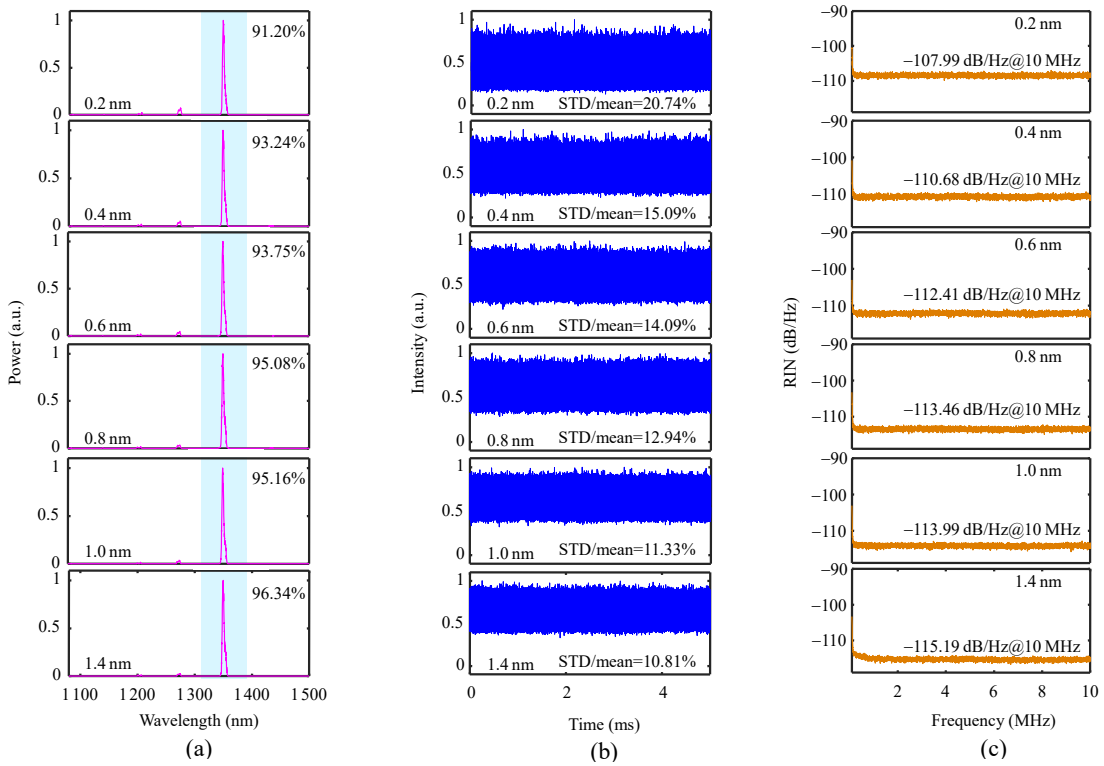

Fig. 6 Properties of the 4th-order random Raman lasing pumped by YRFL with different point reflector's bandwidths: (a) spectra evolution, (b) time domain traces, and (c) RINs.

3.3 Tunable wavelength emissions of the CRRFL

The tunability of the CRRFL is tested as well, by adjusting the central wavelength of the filter used in the YRFL. By fixing the bandwidth as 1.4 nm and changing the central wavelengths from 1055 nm to 1095 nm of the point reflector, the lasing wavelength of the YRFL is tuned accordingly and the normalized spectra are shown in Fig. 7(a). Compared to the tunable filtered ASE pump [35], the wavelength tuning range of the proposed YRFL is wider. Thus, the wavelength tuning ranges of each order random lasing in the CRRFL can also be broadened. Since the 1st-order random lasing is unstable, we record the normalized tunable spectra of the 2nd- to 4th-order random lasings in Figs. 7(b), 7(c), and 7(d), indicating the tuning ranges of 1 169 nm – 1 219 nm, 1 233 nm – 1 287 nm, and 1304 nm – 1364 nm, respectively. The left peaks of several random lasing spectrum in the Fig. 7(b) is caused by another Raman gain maxima. Further decreasing the YRFL wavelength below 1055 nm, the wavelength of the 1st-order random lasing falls outside the wavelength range of the reflection port of the WDM (1 105 nm – 1 700 nm). It is thus possible to further broaden the wavelength tuning range of the CRRFL and realize gap-free wavelength tuning by using the more suitable WDM [32]. Therefore, cascaded random Raman lasing with the good temporal stability and specific wavelength can be simultaneously obtained by tuning the bandwidth and the wavelength of the YRFL pump.

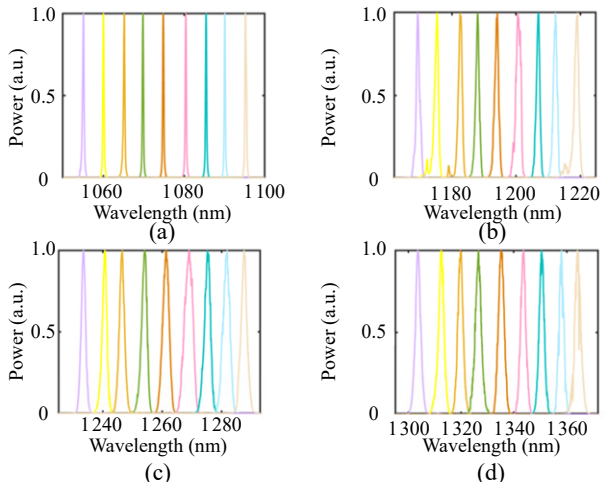

Fig. 7 Normalized spectra of the tunable: (a) YRFL pump, (b) 2nd-, (c) 3rd- and (d) 4th-order random lasings.

4. Conclusions

In summary, we experimentally investigate the impact of the YRFL on the spectral purity and temporal stability of the CRRFL by using a wavelength- and bandwidth-tunable point reflector, for the first time. It is shown that the broader bandwidth of the point reflector in the YRFL leads to the better temporal stability of the YRFL, thus resulting in higher spectral purity and lower RIN of the CRRFL. As a result, with the point reflector's bandwidth of 1.4 nm, a 4th-order CRRFL at 1349 nm with the output power of 3.03 W, spectral purity of 96.34%, and RIN of –115.19 dB/Hz is realized, which is superior to that with 0.2 nm point reflector's bandwidth. Moreover, the wide tunability of the proposed CRRFL is also verified experimentally by continuously tuning the YRFL pump wavelength from 1055 nm to 1095 nm. This work indicates that both the wide wavelength tunability and good temporal stability of the CRRFL can be simultaneously achieved with the broadband random lasing pump, providing a way to further improve distributed Raman amplification pump sources performances by adopting CRRFLs based on the YRFL pump with the broader bandwidth.

Acknowledgment

This work is supported by the key projects of National Natural Science Foundation of China (Grant Nos. 61635005 and U21A20453), and the Zhejiang Lab — UESTC Joint Research Center Project (Grant No. 202012KFY00562).

References

[1] S. K. Turitsyn, S. A. Babin, A. E. El-Taher, P. Harper, D. V. Churkin, S. I. Kablukov, *et al.*, "Random distributed feedback fibre laser," *Nature Photonics*, 2010, 4(4): 231–235.

[2] D. V. Churkin, S. Sugavanam, I. D. Vatnik, Z. Wang, E. Podivilov, S. A. Babin, *et al.*, "Recent advances in fundamentals and applications of random fiber lasers," *Advances in Optics and Photonics*, 2015, 7(3): 516–569.

[3] D. V. Churkin, I.V. Kolokolov, E. V. Podivilov, I. D. Vatnik, M. A. Nikulin, S. S. Vergeles, *et al.*, "Wave kinetics of random fibre lasers," *Nature Communications*, 2015, 6(1): 1–6.

[4] Z. N. Wang, H. Wu, M. Q. Fan, L. Zhang, Y. J. Rao, W. L. Zhang, *et al.*, "High power random fiber laser with short cavity length: theoretical and experimental investigations," *IEEE Journal of Selected Topics in Quantum Electronics*, 2014, 21(1): 10–15.

[5] H. Zhang, L. Huang, J. Song, H. Wu, P. Zhou, X. Wang, *et al.*, "Quasi-kilowatt random fiber laser," *Optics Letters*, 2019, 44(11): 2613–2616.

[6] Z. H. Wang, W. L. Yu, J. D. Tian, T. C. Qi, D. Li, Q. R. Xiao, *et al.*, "5.1 kW tandem-pumped fiber amplifier seeded by random fiber laser with high suppression of stimulated Raman scattering," *IEEE Journal of Quantum Electronics*, 2021, 57(2): 6800109.

[7] L. Zhang, H. W. Jiang, X. Z. Yang, W. W. Pan, S. Z. Cui, and Y. Feng, "Nearly-octave wavelength tuning of a continuous wave fiber laser," *Scientific Reports*, 2017, 7(1): 1–5.

[8] V. Balaswamy, S. Aparanji, S. Arun, S. Ramachandran, and V. R. Supradeepa, "High-power, widely wavelength tunable, grating free Raman fiber laser based on filtered feedback," *Optics Letters*, 2019, 44(2): 279–282.

[9] E. A. Zlobina, S. I. Kablukov, and S. A. Babin, "Linearly polarized random fiber laser with ultimate

efficiency," *Optics Letters*, 2015, 40(17): 4074–4077.

[10] J. X. Song, H. S. Wu, J. Ye, J. M. Xu, H. W. Zhang, and P. Zhou, "High power linearly polarized Raman fiber laser with stable temporal output," *Photonic Sensors*, 2019, 9(1): 43–48.

[11] J. Xu, J. Ye, H. Xiao, J. Leng, W. Liu, and P. Zhou, "In-band pumping avenue based high power superfluorescent fiber source with record power and near-diffraction-limited beam quality," *High Power Laser Science and Engineering*, 2018, 6: E46.

[12] R. Ma, Y. J. Rao, W. L. Zhang, X. Zeng, X. Dong, H. Wu, *et al.*, "Backward supercontinuum generation excited by random lasing," *IEEE Journal of Selected Topics in Quantum Electronics*, 2017, 24(3): 1–5.

[13] J. Ye, J. Xu, H. Zhang, and P. Zhou, "Powerful narrow linewidth random fiber laser," *Photonic Sensors*, 2017, 7(1): 82–87.

[14] J. M. Xu, L. Huang, M. Jiang, J. Ye, P. F. Ma, J. Y. Leng, *et al.*, "Near-diffranction-limited linearly polarized narrow-linewidth random fiber laser with record kilowatt output," *Photonics Research*, 2017, 5(4): 350–354.

[15] A. E. El-Taher, P. Harper, S. A. Babin, D. V. Churkin, E. V. Podivilov, J. D. Ania-Castanon, *et al.*, "Effect of Rayleigh-scattering distributed feedback on multiwavelength Raman fiber laser generation," *Optics Letters*, 2011, 36(2): 130–132.

[16] S. Sugavanam, Z. Yan, V. Kamynin, A. S. Kurkov, L. Zhang, and D. V. Churkin, "Multiwavelength generation in a random distributed feedback fiber laser using an all fiber Lyot filter," *Optics Express*, 2014, 22(3): 2839–2844.

[17] H. Wu, W. Wang, Y. Li, C. Li, J. Yao, Z. Wang, *et al.*, "Difference-frequency generation of random fiber lasers for broadly tunable mid-infrared continuous-wave random lasing generation," *Journal of Lightwave Technology*, DOI: 10.1109/JLT.2022.3148769.

[18] J. Xu, J. Ye, W. Liu, J. Wu, H. Zhang, J. Leng, *et al.*, "Passively spatiotemporal gain-modulation-induced stable pulsing operation of a random fiber laser," *Photonics Research*, 2017, 5(6): 598–603.

[19] N. Tarasov, L. A. Melnikov, I. D. Vatnik, Y. A. Mazhirina, and D. V. Churkin, "Self-gain-modulation random distributed feedback Raman fiber laser with switchable repetition rate," *Optics Letters*, 2021, 29(19): 29857–29863.

[20] M. Tan, P. Rosa, S. T. Le, Md. A. Iqbal, I. D. Phillips, and P. Harper, "Transmission performance improvement using random DFB laser based Raman amplification and bidirectional second-order pumping," *Optics Express*, 2016, 24(3): 2215–2221.

[21] Z. N. Wang, Y. J. Rao, H. Wu, P. Li, Y. Jiang, X. H. Jia, *et al.*, "Long-distance fiber-optic point-sensing systems based on random fiber laser," *Optics Express*, 2012, 20(16): 17695–17700.

[22] Z. N. Wang, W. Sun, H. Wu, X. Y. Qian, Q. H. He, Z. D. Wei, *et al.*, "Long-distance random fiber laser point sensing system incorporating active fiber," *Optics Express*, 2016, 24(20): 22448–22453.

[23] X. Jia, Y. Rao, C. Yuan, J. Li, X. Yan, Z. Wang, *et al.*, "Hybrid distributed Raman amplification combining random fiber laser based 2nd-order and low-noise LD based 1st-order pumping," *Optics Express*, 2013, 21(21): 24611–24619.

[24] Y. Fu, R. C. Zhu, B. Han, H. Wu, Y. J. Rao, C. Y. Lu, *et al.*, "175-km repeaterless BOTDA with hybrid high-order random fiber laser amplification," *Journal of Lightwave Technology*, 2019, 37(18): 4680–4686.

[25] H. Wu, B. Han, Z. N. Wang, G. Genty, G. Y. Feng, and H. K. Liang, "Temporal ghost imaging with random fiber lasers," *Optics Express*, 2020, 28(7): 9957–9964.

[26] J. Y. Guo, Y. J. Rao, W. L. Zhang, Z. W. Cui, A. R. Liu, and Y. M. Yan, "Dental imaging with near-infrared transillumination using random fiber laser," *Photonic Sensors*, 2020, 10(4): 333–339.

[27] E. I. Dontsova, S. I. Kablukov, I. D. Vatnik, and S. A. Babin, "Frequency doubling of Raman fiber lasers with random distributed feedback," *Optics Letters*, 2016, 41(7): 1439–1442.

[28] S. Z. Cui, J. P. Qian, X. Zeng, X. Cheng, X. J. Gu, and Y, Feng, "A watt-level yellow random laser via single-pass frequency doubling of a random Raman fiber laser," *Optical Fiber Technology*, 2021, 64: 102552.

[29] V. Balaswamy, S. Ramachandran, and V. R. Supradeepa, "High-power, cascaded random Raman fiber laser with near complete conversion over wide wavelength and power tuning," *Optics Express*, 2019, 27(7): 9725–9732.

[30] S. A. Babin, I. D. Vatnik, A. Yu. Laptev, M. M. Bubnov, and E. M. Dianov, "High-efficiency cascaded Raman fiber laser with random distributed feedback," *Optics Express*, 2014, 22(21): 24929–24934.

[31] I. D. Vatnik, D. V. Churkin, S. A. Babin, and S. K. Turitsyn, "Cascaded random distributed feedback Raman fiber laser operating at 1.2 μm," *Optics Express*, 2011, 19(19): 18486–18494.

[32] L. Zhang, J. Y. Dong, and Y. Feng, "High-power and high-order random Raman fiber lasers," *IEEE Journal of Selected Topics in Quantum Electronics*, 2017, 24(3): 1–6.

[33] J. Y. Dong, L. Zhang, H. W. Jiang, X. Z. Yang, W. W. Pan, S. Z. Cui, *et al.*, "High order cascaded Raman random fiber laser with high spectral purity," *Optics Express*, 2018, 26(5): 5275–5280.

[34] J. Ye, J. M. Xu, J. X. Song, Y. Zhang, H. W. Zhang, H. Xiao, *et al.*, "Pump scheme optimization of an incoherently pumped high-power random fiber laser," *Photonics Research*, 2019, 7(9): 977–983.

[35] Y. Zhang, J. X. Song, J. Ye, J. M. Xu, T. F. Yao, and P. Zhou, "Tunable random Raman fiber laser at 1.7 μm region with high spectral purity," *Optics Express*, 2019, 27(20): 28800–28807.
[36] H. Wu, Z. Wang, Q. He, W. Sun, and Y. Rao, "Common-cavity ytterbium/Raman random distributed feedback fiber laser," *Laser Physics Letters*, 2017, 14(6): 065101.
[37] B. Han, Y. J. Rao, H. Wu, J. Z. Yao, H. J. Guan, R. Ma, *et al.*, "Low-noise high-order Raman fiber laser pumped by random lasing," *Optics Letters*, 2020, 45(20): 5804–5807.
[38] X. Y. Du, H. W. Zhang, X. L. Wang, and P. Zhou, "Tunable random distributed feedback fiber laser operating at 1 μm," *Applied optics*, 2015, 54(4): 908–911.
[39] S. Sugavanam, N. Tarasov, X. Shu, and D. V. Churkin, "Narrow-band generation in random distributed feedback fiber laser," *Optics Express*, 2013, 21(14): 16466–16472.
[40] H. Wu, B. Han, and Y. Liu, "Tunable narrowband cascaded random Raman fiber laser," *Optics Express*, 2021, 29(14): 21539–21550.
[41] D. V. Churkin and S. V. Smirnov. "Numerical modelling of spectral, temporal and statistical properties of Raman fiber laser," *Optics Communications*, 2012, 285(8): 2154–2160.
[42] S. V. Smirnov and D. V. Churkin. "Modeling of spectral and statistical properties of a random distributed feedback fiber laser," *Optics Express*, 2013, 21(18): 21236–21241.
[43] J. Nuno, M. Alcon-Camas, and J. D. Ania-Castanon, "RIN transfer in random distributed feedback fiber lasers," *Optics Express*, 2012, 20(24): 27376–27381.